Available online at www.sciencedirect.com
SCIENCE DIRECT®
Earth and Planetary Science Letters 240 (2005) 205–220
EPSL
www.elsevier.com/locate/epsl

What are the climate controls on δD in precipitation in the Zongo Valley (Bolivia)? Implications for the Illimani ice core interpretation

Françoise Vimeux [a,*], Robert Gallaire [b], Sandrine Bony [c], Georg Hoffmann [d], John C.H. Chiang [e]

[a] IRD, UR 032 Great Ice-IPSL/Laboratoire des Sciences du Climat et de l'Environnement, CE Saclay, Orme des Merisiers, Bât. 709, 91191 Gif-sur-Yvette Cedex, France
[b] IRD, UR 032 Great Ice-Senamhi-La Mariscala 115 San Isidro, Lima, Peru
[c] IPSL/Laboratoire de Météorologie Dynamique, 2 place Jussieu 75252 Paris Cedex 10, France
[d] IPSL/Laboratoire des Sciences du Climat et de l'Environnement, CE Saclay, Orme des Merisiers, Bât. 709, 91191 Gif-sur-Yvette Cedex, France
[e] Department of Geography and Center for Atmospheric Sciences, University of California, Berkeley, CA 94720-4740, USA

Received 15 March 2005; received in revised form 13 July 2005; accepted 19 September 2005
Available online 21 October 2005
Editor: E. Boyle

Abstract

Controversy has surrounded the interpretation of the water isotopic composition (δD or δ^{18}O) in tropical and subtropical ice cores in South America. Although recent modeling studies using AGCM have provided useful constraints at interannual time scales, no direct calibration based on modern observations has been achieved. In the context of the recent ice core drilling at Nevado Illimani (16°39′S–67°47′W) in Bolivia, we examine the climatic controls on the modern isotopic composition of precipitation in the Zongo Valley, located on the northeast side of the Cordillera Real, at about 55 km from Nevado Illimani. Monthly precipitation samples were collected from September 1999 to August 2004 at various altitudes along this valley. First we examine the local and regional controls on the common δD signal measured along this valley. We show that (1) local temperature has definitely no control on δD variations, and (2) local rainout is a poor factor to explain δD variations. We thus seek regional controls upstream the Valley potentially affecting air masses distillation. Based on backtrajectory calculations and using satellite data (TRMM precipitation, NOAA OLR) and direct observations of precipitation (IAEA/GNIP), we show that moisture transport history and the degree of rainout upstream are more important factors explaining seasonal δD variations. Analysis of a 92-yr simulation from the ECHAM-4 model (T30 version) implemented with water stable isotopes confirms our observations at seasonal time scale and emphasize the role of air masses distillation upstream as a prominent factor controlling interannual δD variations. Lastly, we focus on the isotopic depletion along the valley when air masses are lifted up. Our results suggest that, if the temperature gradient between the base and the top of the Andes was higher by a few degrees during the Last Glacial Maximum (LGM), less than 10% of the glacial to interglacial isotopic variation recorded in the Illimani ice core could be accounted for by this temperature change. It implies that the rest of the variation would originate from wetter conditions along air masses trajectory during LGM.

Keywords: South America; Andes; water stable isotopes; calibration; ice cores; glacial–interglacial transition

* Corresponding author. Tel.: +33 1 69 08 57 71; fax: +33 1 69 08 77 16.
E-mail address: vimeux@lsce.saclay.cea.fr (F. Vimeux).

0012-821X/$ - see front matter
doi:10.1016/j.epsl.2005.09.031

1. Introduction

1.1. Background and motivations

There has been important attempts at documenting past climate variability of tropical areas over the last decade. For example, a number of tropical and subtropical ice cores has been drilled along the Andes of South America between 10° and 18°S. Water stable isotopes (δD or δ^{18}O, hereafter δ) have been measured on those ice cores and several isotopic records are now available back to the Last Glacial Maximum (LGM) [1–4]. In Antarctica, the isotopic composition of ice has provided robust paleotemperature reconstructions by using the modern linear covariance between condensation temperature and isotopic composition of precipitation [5,6]. Indeed, the isotopic composition of precipitation primarily records the rainout history of air masses which is intimately related to the condensation temperature via the Clausius–Clapeyron equation [7]. However, in tropical regions, the atmospheric cycle of water isotopes is much more complex and atmospheric temperature variations are not entirely related to condensation. Actually, most of precipitation depends on small-scale vertical convection so that the first-order estimate of the degree of distillation is not the condensation temperature and the δ/T covariance breaks down. Therefore, the rainout becomes the dominant control on isotopic composition, known as “the amount effect” [8,9].

Other “path effects” affect the isotopic composition of precipitation in tropical South America: seasonal change of ocean moisture source regions, fractionating versus non-fractionating recycling over Amazonia, partial re-evaporation of droplets during fall or at the base of clouds and re-equilibration with surrounding vapor, orographic obstacles inducing adiabatic cooling and precipitation. Given this uncertainty, conflicting interpretations have emerged on the causes of past variability of δ in the Andean ice cores. δ records have been interpreted in a similar way to those from higher latitudes in terms of temperature changes [3] or as reflecting precipitation amount changes over Amazonia [4]. Recently, some studies have explored the effects of the El Niño-Southern Oscillation (ENSO) to reconcile the different interpretations. They proposed that Equatorial Pacific Sea Surface Temperatures (hereafter, SSTs) variations can remotely control Amazon precipitation and hence the isotopic composition of Andean ice cores [10–13].

Modeling studies using Atmospheric Global Circulation Model (hereafter, AGCM) implemented with water stable isotopes have tried to solve the conflict by exploring the climate controls on modern isotopic composition of precipitation. A significant dependence of isotopes on a combination of factors is shown with an emphasis on the role of precipitation amount for most of tropical South American regions [14–16]. Some isolated studies on water vapor samples have shown a significant impact of storm activity on δ [17,18].

However, a direct isotopic calibration based on modern observations is still missing to reliably interpret Andean ice cores. Thus, IRD (Institut de Recherche pour le Développement) has set up a network monitoring monthly and daily isotopic composition of precipitation in Bolivia, Peru and Ecuador since 1999. We focus in this paper on the controls of specific isotopic composition of Bolivian precipitation that might help us to better interpret the Illimani ice core [4]. We examine local and regional climate controls on δ variations and discuss the consequences for the Illimani ice core interpretation.

1.2. Collecting site: the Zongo Valley (Bolivia)

We present in this paper the isotopic composition (δD) of monthly precipitation collected in Bolivia along the Zongo Valley (16°20′S, 67°47′W) from September 1999 to August 2004. This Valley, linking the Amazon basin to the Bolivian Altiplano, is located on the northeast side of the Bolivian Cordillera Real—55 km northwesterly from Nevado Illimani (16°39′S, 67°47′W, ~6300 m) where an ice core was drilled in 1999 [4,13] (Fig. 1). The Cordillera Real is the first major orographic obstacle encountered by air masses that originate from the Atlantic Ocean and are recycled intensely over the Amazon basin (about 50%) [19,20] before they move up the Andes and precipitate (see next section for air parcel pathways). Thus, monitoring the isotopic composition of precipitation along this valley enables one to study (1) the isotopic composition of precipitation right after the Amazon portion of the air parcels path and (2) the isotopic depletion of precipitation when air masses lift up the Andes. It thus offers a unique opportunity to investigate the δ variability of modern precipitation in order to refine the interpretation of the Illimani δ record.

Since September 1999, five pluviometers have been collecting monthly precipitation along this valley at the sites named Harca (1480 m); Sainani (2210 m);

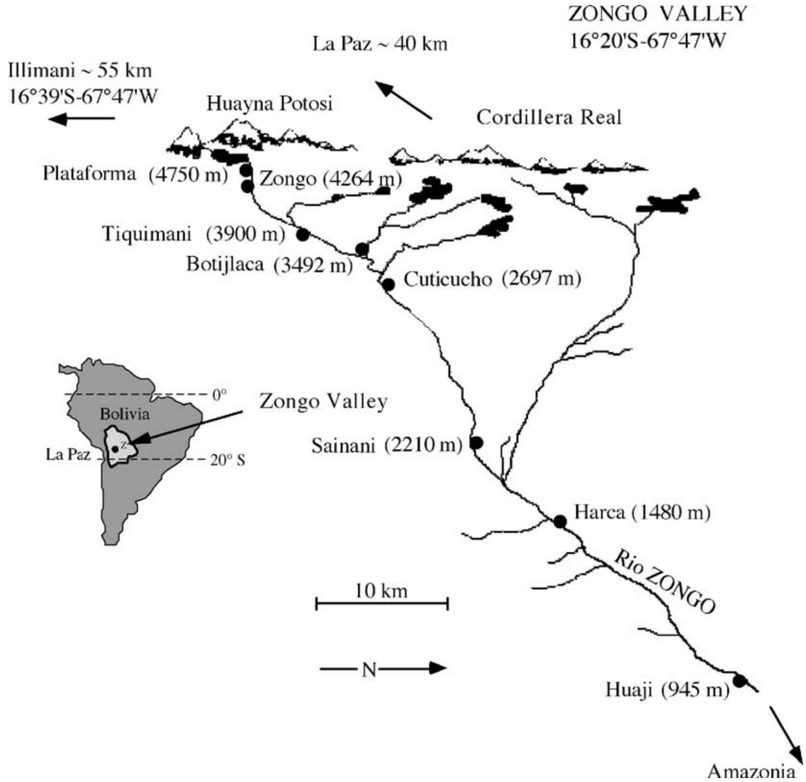

Fig. 1. Map of the Zongo Valley (Bolivia) with the locations of the 8 pluviometers at Huaji (945 m), Harca (1480 m), Sainami (2210 m), Cuticucho (2697 m), Botijlaca (3492 m), Tiquimani (3900 m), Zongo (4264 m) and Plataforma (4750 m).

Botijlaca (3492 m); Tiquimani (3900 m) and Zongo (4264 m). Over the first 12 months, precipitation was also collected on a based-event resolution (precipitation >2 mm) at the same places and at 3 additional stations at intermediate elevations: Huaji (945 m); Cuticucho (2697 m) and Plataforma (4750 m). This valley belongs to the Bolivian Company of Electric Energy (COBEE) providing electric power for La Paz and all pluviometers are located nearby the hydropower plants. The proximity of the hydropower plants allowed us to have dedicated observers that monitored the pluviometers throughout the year, guaranteeing the quality of the observations. Precipitation amount is directly read on pluviometers. For temperature, three captors are located in the valley at 945 m, 2697 m and 4750 m and measure 2-m surface temperature. Only the captor at the highest elevation recorded temperature variations over the entire period of our observations; the others started recording temperature in January 2002. Over the overlapping period (January 2002–August 2004), monthly temperature variations between the base and the top of the valley clearly evolve in parallel ($r^2=0.75$, significant at 99.9%, hereafter $p=0.001$) with a nearly constant difference of 19 °C ($\sigma_{n=32}=1$ °C). Thus, temperature variations can be estimated at each station using the mean along-slope lapse rate (0.49 ± 0.03 °C/100 m).

To check that the isotopic composition of precipitation in this valley is linked to the isotopic seasonal signal of precipitation falling on Nevado Illimani, we performed in October 2002 two 2-m snow pit measurements: at Illimani on the site of the deep ice core drilling and on the Huayna Potosi up the Zongo Valley (5810 m) (Fig. 1). δ^{18}O measurements show different accumulation rates (also shown by chemical species analysis, F. Delachaux, pers. comm.) and the covered period is about 1.5 yr and 1 yr at Illimani and Huayna respectively (not shown). Over the overlapping period, δ^{18}O records exhibit similar isotopic variations ($r^2=0.85$, $p<0.001$), with a comparable seasonal variation ($\Delta\delta^{18}O_{Huayna}=15.9$ ‰; $\Delta\delta^{18}O_{Illimani}=17$ ‰; this difference can be explained by the 500-m altitude difference, see next section) and a similar mean over the common period ($\delta^{18}O_{Huayna}=-14.9$ ‰ and $\delta^{18}O_{Illimani}=-14.3$ ‰). We are aware that this test lies only on 1 yr and should be double-checked over a longer period; however, we are confident about its linkage to the δ variability in the Zongo Valley given the proximity of both sites.

2. Results and discussion on climate controls on δ

All δD measurements are performed with an accuracy of ±0.5‰. The 5-yr-long monthly records are presented in Fig. 2 along with precipitation amount and temperature variations (only for the lowest station). Two major observations can be made:

- δD signals are fairly similar from one station to another, exhibiting a clear seasonal cycle with the most depleted values within the wet season (between January and March) and the most enriched values within the dry season (between July and September) (Fig. 2). This is confirmed by a Principal Component Analysis (PCA) performed on the five δD records providing as a first component a combination explaining 91% of the variance. Thus, in Section 2.1, we will explore what are the climate controls on the common δD variations, independently on the site of collection in the valley.
- As expected, δD values are depleted with altitude. In Section 2.2, we will examine how the δD signal evolves along the valley when air masses are lifted up in the Andes (is it a classical Rayleigh distillation?).

2.1. Influence of local and regional climate parameters on δD at seasonal and interannual time scale

In the next two subsections, we focus on seasonal δD variability. The interannual δD variability is examined in the third subsection.

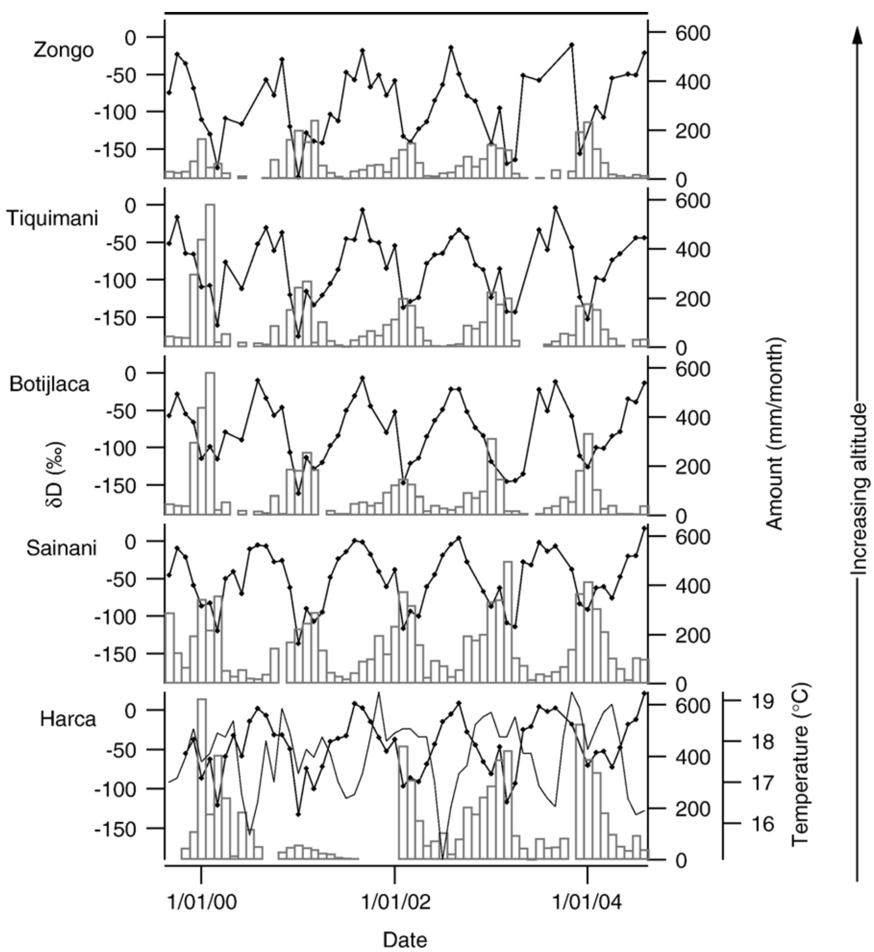

Fig. 2. Monthly δD variations (in ‰ relative to SMOW) from September 1999 to August 2004 for Harca, Sainani, Botijlaca, Tiquimani and Zongo stations (solid line with markers) along with precipitation variations (bars, mm/month) and temperature (°C) for Harca (solid line) (as temperature is based on one record and calculated with the calculated lapse rate, see text, it is only shown for Harca station).

2.1.1. Local controls?

Given the similarity between the five monthly δD records, we calculate the mean 5-yr-long weighted isotopic signal (δD_{Zongo}) and examine the correlations with the mean local precipitation (P_{Zongo}) and temperature (T_{Zongo}) (Fig. 3a).

The δD_{Zongo}–T_{Zongo} relationship is negative (Fig. 3b and Table 1) that cannot be explained by our current understanding of water isotopic fractionation. As already noted by Rozanski and Araguas-Araguas [9], a negative relationship between isotopes and temperature often appears in tropical regions because high temperatures and rainy season tend to coincide.

The δD_{Zongo} covariation with P_{Zongo} (r^2) is 0.48 ($p<0.001$) suggesting that about half of the isotopic variations could be explained by the local rainout (Fig. 3c). We note that the use of a mean signal largely overestimates the individual $\delta D/P$ correlation ranging from 0.15 to 0.48 (see Table 1). It is noteworthy that δD_{Zongo} attains its more depleted value in January 2001, during a wet period classified as a weak La Niña year, while local precipitation attains its minimum, contradicting the well known amount effect.

Two intriguing observations in the δD_{Zongo}–P_{Zongo} relationship are worth discussing. First, the strength of the correlation is highly variable from one station to the next and this can be assigned to precipitation discrepancies along the valley (a principal component analysis performed on the precipitation records provides as a first component a combination explaining 73% of the variance compared to 91% for the isotopic record), already observed on a longer time scale in this valley by Pouyaud et al. and Ronchail and Gallaire [21,22]. Second, we note a sizeable scattering of isotopic values for low precipitation (under ~120 mm) (Fig. 3c). If we focus on the wet season only (November–April), the covariance is found to decrease down to 0.26. Over the dry season (May–October), the correlation is not significant ($r^2=0.01$), simply reflecting the low and constant precipitation level of P_{Zongo} whereas δD_{Zongo} exhibits a large variation, suggesting that local rainout cannot explain the wintertime δ enrichment.

Thus, to further evaluate whether the correlation between δD_{Zongo} and P_{Zongo} is robust with respect to the fact that both P_{Zongo} and δD_{Zongo} have a strong seasonal cycle (certainly largely explaining the magnitude of the covariance), we examine the event-based

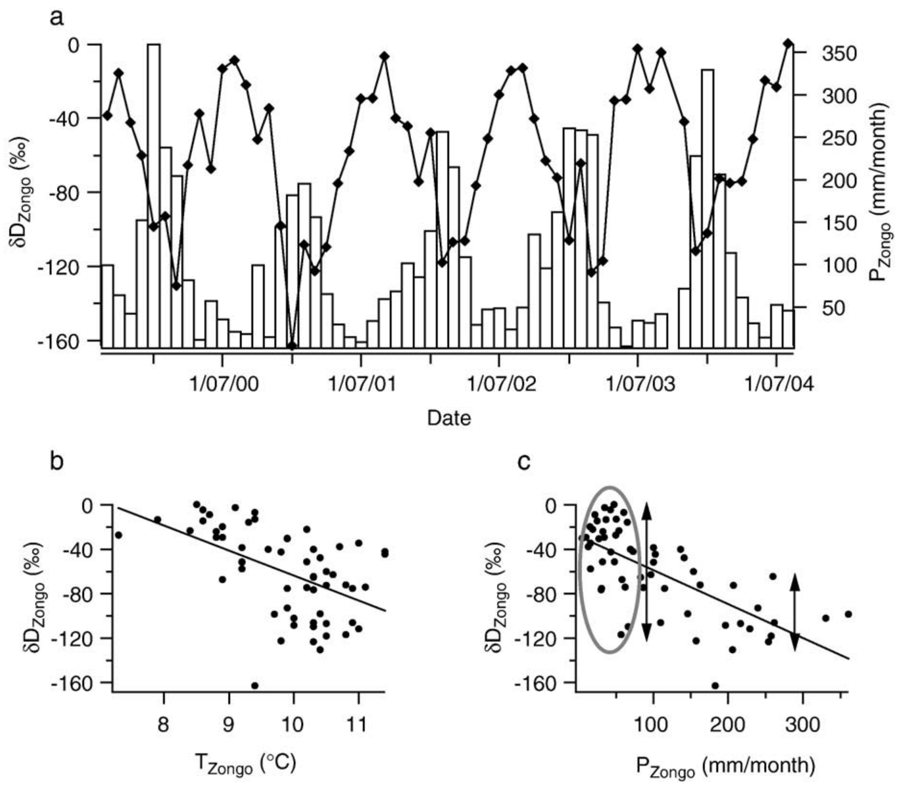

Fig. 3. (a) Weighted δD_{Zongo} (in ‰ relative to SMOW) from September 1999 to August 2004 along with mean precipitation in the valley (P_{Zongo}, mm/month); (b) scatter plot between δD_{Zongo} and mean temperature in the Valley T_{Zongo} (°C); (c) scatter plot between δD_{Zongo} and P_{Zongo}.

Table 1
Covariance (r^2) and slope between δD and precipitation and temperature for each station in the Zongo Valley from September 1999 to August 2004

Stations	Slope $\delta D/P$ (‰/mm)	r^2 $\delta D/P$ ($r<0$)	Slope $\delta D/T$ (‰/°C)	r^2 $\delta D/T$ ($r<0$)
Harca	− 0.13	0.27	− 19.34	0.23
Sainani	− 0.17	0.48	− 22.60	0.28
Botijlaca	− 0.21	0.15	− 25.18	0.28
Tiquimani	− 0.34	0.39	− 18.68	0.15
Zongo	− 0.46	0.36	− 15.99	0.09

We remind that a 5-yr (60-point) correlation is significant at the 99.9% level when $r^2=0.17$.

isotopic composition of precipitation collected from September 1999 to August 2000 (not shown). Over this period, each precipitation event higher than 2 mm (excluding potential precipitation altered by partial evaporation of droplets during fall) was collected and analyzed for deuterium. δD records are fairly similar from one station to another (the first component of a PCA accounts for 89% of the variance) and clearly show an intra-month variability superimposed on the seasonal trend. Conversely, the precipitation distribution over the whole year and occurrence and distribution of large events largely differ from one station to another (the first EOF of a PCA accounts for only 36% of the variance). The precipitation discrepancies relative to the common δD signal clearly reveals that individual precipitation has no control on δ. Actually, the δ/P covariance (r^2) never exceeds 0.05 except for the lowest station where $r^2=0.15$. Those scatter plots (not shown) clearly evidence a large scattering of isotopic values for weak precipitation (<20–40 mm, depending

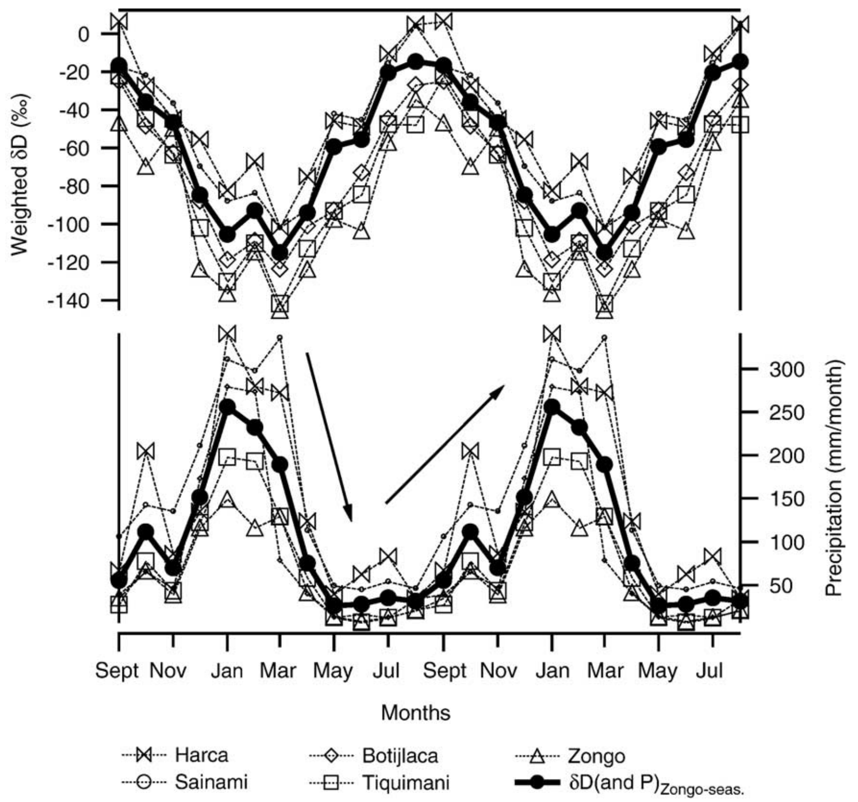

Fig. 4. Mean precipitation and weighted δD seasonal cycle at Harca, Sainani, Botijlaca, Tiquimani and Zongo (dotted lines with markers). A weighted isotopic signal has been extracted ($\delta D_{\text{Zongo-seasonal}}$) as well as a mean precipitation signal ($P_{\text{Zongo-seasonal}}$) (black curves and circles). Arrows indicate the abrupt precipitation transition into the dry season compared to the weaker one into the wet season. Two seasonal cycles are shown to clearly illustrate the dry-to-wet season transition.

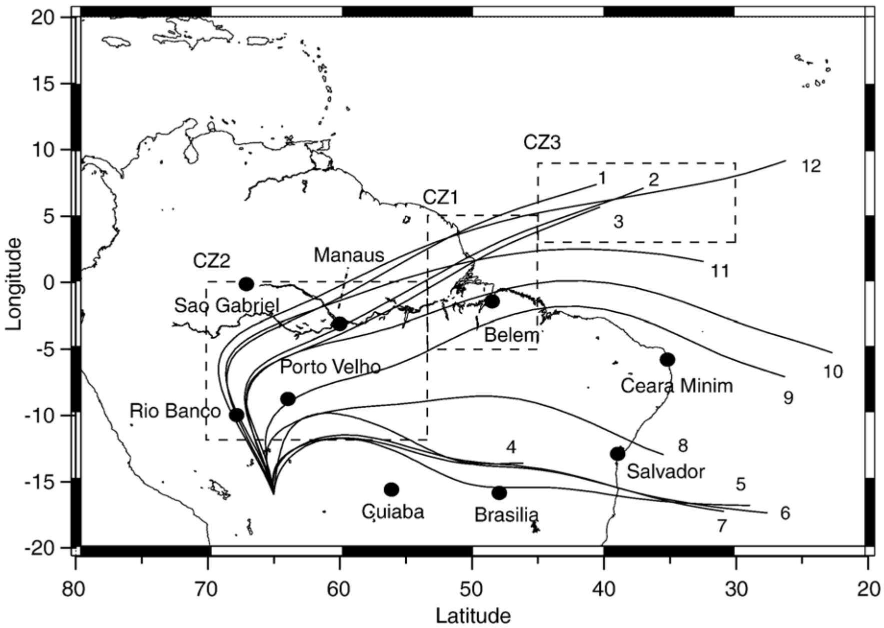

Fig. 5. Backtrajectories from January (1) to December (12). Black circles show location of IAEA/GNIP stations used in this study. The stations located nearby the "wet" pathways and used to calculate P_{wet} are: Belem, Manaus, Sao Gabriel, Porto Vehlo and Rio Banco. The stations located nearby the "dry" pathways and used to calculate P_{dry} are: Salvador, Cearaminim, Brasilia and Cuira). The "Amazon group" considers all previous stations together. Convective zones (CZ1, 2 and 3) are indicated (rectangles with dotted lines).

on the altitude), present all over the year, so that the weighted isotopic monthly values are biased by the larger occurrence of important precipitation events during the wet season and a clear antiphase appears between isotope and precipitation seasonal cycle.

The main point arising from those calculations is that local rainout (and temperature) is insufficient to explain many aspects of δD variability in precipitation at the base of the Cordillera Real. In the next section, we examine the influence of moisture transport history and the degree of rainout upstream as potential important factors to explain seasonal δD variations.

2.1.2. Regional controls?

In this section, we aim at comparing δD variability in the valley as a whole with precipitation regime upstream. Indeed, we know that the isotopic composition of precipitation reflects integrated climate information from the oceanic moisture sources to the site of collection.

As an initial exploration, we compare $\delta D_{\mathrm{Zongo}}$ with precipitation data from the IAEA/GNIP (International Atomic Energy Agency/Global Network of Isotopes in Precipitation) network [23] available until 2001 at monthly resolution. As those observations do not cover the same period as our isotopic records, we calculate the mean seasonal cycle for both isotopes and precipitation in the valley ($\delta D_{\mathrm{Zongo\text{-}seasonal}}$ and $P_{\mathrm{Zongo\text{-}seasonal}}$) (Fig. 4) and compare it with the mean seasonal cycle of IAEA/GNIP precipitation. We are aware that this method implies comparison of two parameters (δ and P) with a strong seasonal cycle likely responsible for an important part of the covariance magnitude. Thus, we will only discuss 12-point (or 6-point) correlations significant at $p<0.001$, i.e. $r^2>0.68$ ($p<0.01$, $r^2>0.84$).

The $\delta D_{\mathrm{Zongo\text{-}seasonal}}/P_{\mathrm{Zongo\text{-}seasonal}}$ correlation is 0.57. The correlation is found to decrease to 0.42 over the wet season (November–April) and to 0.02 over the dry season (March–October).

To provide a comparison that makes sense, it is necessary to select stations located nearby the trajectories of air masses and preferably where deep convection occurs. So first, using different re-analyses and satellite data sets, we compute backtrajectories of the air masses and locate deep convective activity along those pathways.

Backtrajectories have been computed for each month. The end point is the base of the Zongo Valley and robustness of trajectories to its small spatial displacements ($\pm 1.5^{\circ}$ of longitude) has been checked. Wind fields are taken from NCEP–NCAR (National Centers for Environmental Prediction–National Center for Atmospheric Research) re-analyses climatological

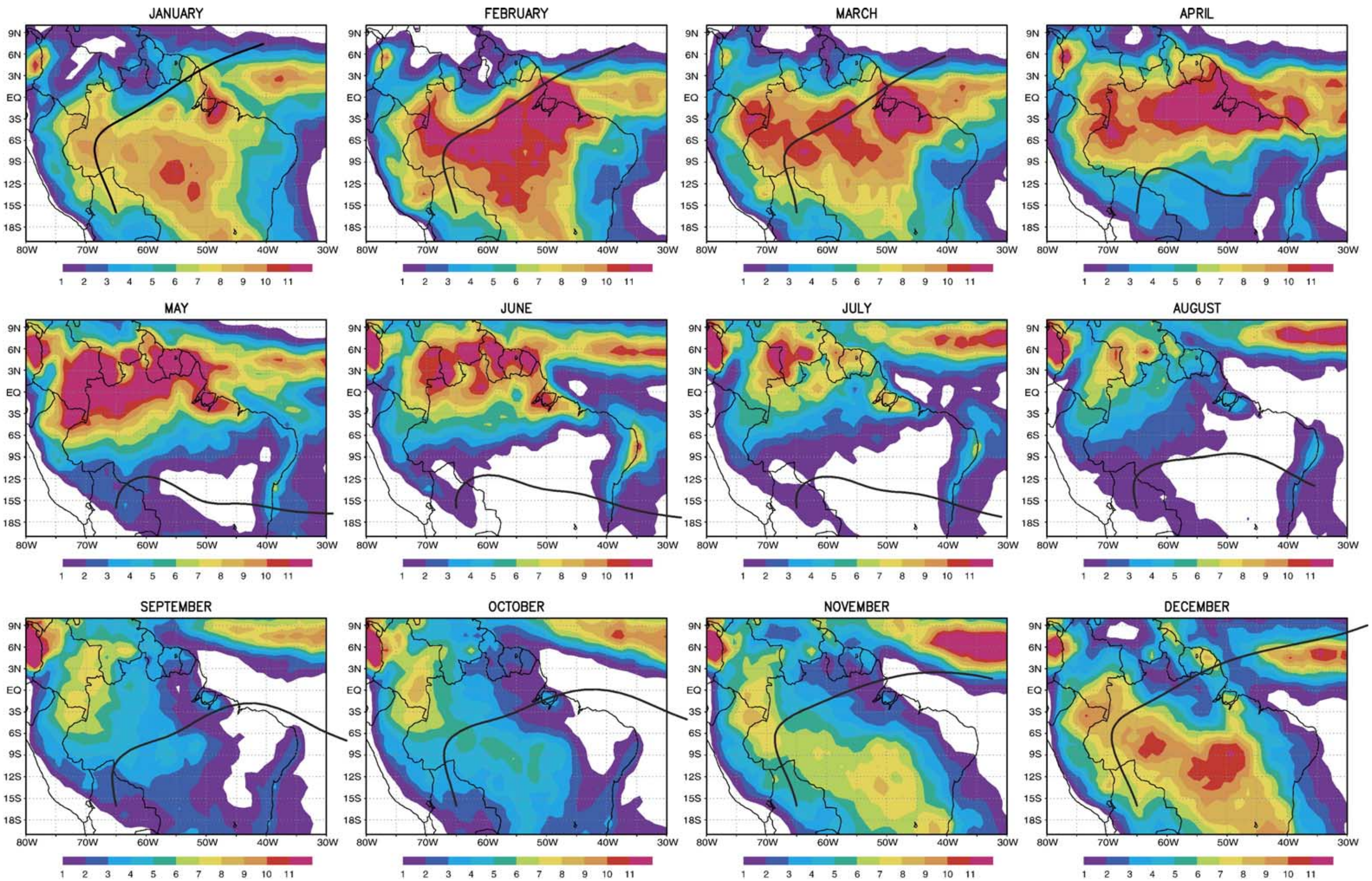

Fig. 6. TRMM precipitation (mm/day) distribution averaged for each month from September 1999 to March 2004 along with backtrajectories.

monthly means [24]. The later are averaged over the 1979–2002 time period, and the winds used are mass-weighted vertical averages over 850–1000 mb. Indeed, the moisture transport leading up to the central Andes occurs in near-surface levels [25] where moisture content is maximum. Backtrajectories are computed with a predictor–corrector method using a 1-h timestep until the trajectories reach the Atlantic Ocean or back to 19 days. Concerning the wintertime precipitation, we do not take into account that winter storm tracks may be able to penetrate as northward as the Zongo Valley. We also tested the representativeness of a mean backtrajectory calculation over 23 yr by checking that trajectories for El Niño and La Niña conditions are not drastically different. Backtrajectories are plotted in Fig. 5. As expected, the primary moisture source is the tropical Atlantic Ocean via the Amazon Basin and the air masses pathway is entirely controlled by the marine ITCZ (InterTropical Convergence Zone) seasonal displacement. A clear separation between winter trajectories (April–August) and summer trajectories (November–March) is shown with an intermediate position for September and October. The abrupt shift between March and April trajectories is consistent with the abrupt transition into the dry season compared to the gradual change to the wet period (see arrows in Fig. 4). It takes about 10 (more than 14) days for the water vapor parcel to travel from the Atlantic Ocean to the base of the Andes during the wet season (dry season). We note also that the air parcel speed is lower as air masses penetrate into the continent, specifically for wintertime trajectories (more than 5 days following the Andes) (not shown). As the travel time of air parcels is lower than a month, it makes sense to study a monthly based comparison between isotopes in the Zongo Valley and precipitation along the trajectories.

To examine where convective activity occurs upstream the Zongo Valley, we use merged satellite precipitation data set acquired as part of the Tropical Rainfall Measuring Mission (TRMM) [26] from September 1999 to March 2004 (resolution of $1^\circ \times 1^\circ$), nearly corresponding to the time period of our observations (data are not available until August 2004 yet). The spatial distribution robustness of TRMM precipitation is checked with other satellite data sets: GPCP (Global Precipitation Climatology Project [27]), and CMAP (CPC Merged Analysis Precipitation [28]), data sets covering the longer 1979–1999 period indicate a similar spatial distribution of large scale convective activity (not shown). We show in Fig. 6 TRMM precipitation maps as well as backtrajectories for each month. From November to March, air masses undergo a strong convective activity all along the trajectory. Two important convective zones are shown: the Convective Zone 1 (CZ1) located over the 5°N–5°S/45–53°W region and the Convective Zone 2 (CZ2) located over the 0–12°S/53–70°W region (Fig. 5). We also note that from November to January, a third convective area (CZ3) located over the 3–9°N/30–45°W region could account for initial low isotopic composition of precipitation (Fig. 5). From April to August, precipitation is fairly low and constant over the Amazon portion of the air masses trajectory and the major precipitation zone is located at the edge of the continent.

Considering backtrajectory calculations and precipitation distribution, we choose 9 IAEA/GNIP stations, having at least 3 yr of information and plotted in Fig. 5. If we calculate a mean precipitation seasonal cycle (P_{Amazon}) from the 9 stations, the $\delta D_{Zongo\text{-}seasonal}/P_{Amazon}$ correlation is found to increase to 0.91 (r^2) (Table 2). Individual correlations are found to be lower (mean effect) and maximum with stations located nearby the austral summer trajectories (Manaus, 0.86; Belem, 0.84 and Rio Banco, 0.75). Therefore, $\delta D_{Zongo\text{-}seasonal}$ would be more controlled by the intense Amazon convection upstream the valley over the wet season. Specifically, the two major convective zones revealed by TRMM precipitation distribution seem to be involved: CZ1 centered on the Belem station and CZ2 eastwards near Rio Banco station where trajectories start following the Andes southwards with a highly reduced speed possibly

Table 2
Covariance (r^2) between δD_{zongo} (5-yr-long signal) and/or $\delta D_{Zongo\text{-}seasonal}$ (1-yr-long signal) and local precipitation (P_{Zongo} and $P_{Zongo\text{-}Seasonal}$ as defined in the text), IAEA/GNIP precipitation over Amazonia (9 IAEA/GNIP stations combined to define P_{Amazon}, see the text and the legend of Fig. 5), TRMM precipitation between September 1999 and March 2004, and OLR

	P_{Zongo}	$P_{Zongo\text{-}Seas.}$	P_{Amazon}	$P_{TRMM\text{-}Zongo}$	$P_{TRMM\text{-}Amazon}$	OLR_{Zongo}	OLR_{Amazon}
δD_{zongo}	0.48 (−0.31)	–	–	0.55 (−0.53)	0.64 (−0.46)	0.32	0.52
$\delta D_{Zongo\text{-}seasonal}$	–	0.57 (−0.33)	0.91 (−0.55)	–	–	0.47	0.70

For TRMM precipitation and OLR, data are averaged over 2 regions: the Zongo (15–20°S/61–66°W) and Amazonia (5°N–18°S/35–70°W). Slopes of the linear regressions with precipitation are indicated in brackets (‰/mm). We remind that a seasonal (12-point) correlation is significant at the 99.9% level when $r^2=0.68$.

explaining the influence of this second zone on air masses distillation. Again, considering separately the wet (November–April) and the dry (May–October) season as defined in the previous section, the $\delta D_{\text{Zongo-seasonal}}/P_{\text{Amazon}}$ correlation is found to be 0.79 and 0.70 respectively ($p<0.05$), that is significant conversely to the $\delta D_{\text{Zongo-seasonal}}/P_{\text{Zongo-seasonal}}$ correlation, insignificant when wet and dry seasons are considered separately. However, all the later correlations involving P_{Amazon} do not account for the southward shift of moisture transport during wintertime. Thus, we calculate two precipitation seasonal cycles (P_{wet} and P_{dry}) averaging precipitation in stations located nearby the "wet" and the "dry" pathways respectively (see legend of Fig. 5) and we examine the correlations with $\delta D_{\text{Zongo-seasonal}}$. The $\delta D_{\text{Zongo-seasonal}}/P_{\text{wet (dry) group}}$ (6-point) correlation over the wet (dry) season is found to increase to 0.92 (0.86), $p<0.01$. Again, considering individual station, the highest correlation is found over the wet season with Belem and Manaus precipitation (0.81 an 0.78) and over the dry season with Salvador precipitation (0.75) ($p<0.05$) as expected.

Actually, in contrast to Zongo precipitation, eastern Amazon precipitation exhibits a strong seasonal cycle that could explain δD_{Zongo} variations from May to September as clearly shown in Fig. 7 where TRMM

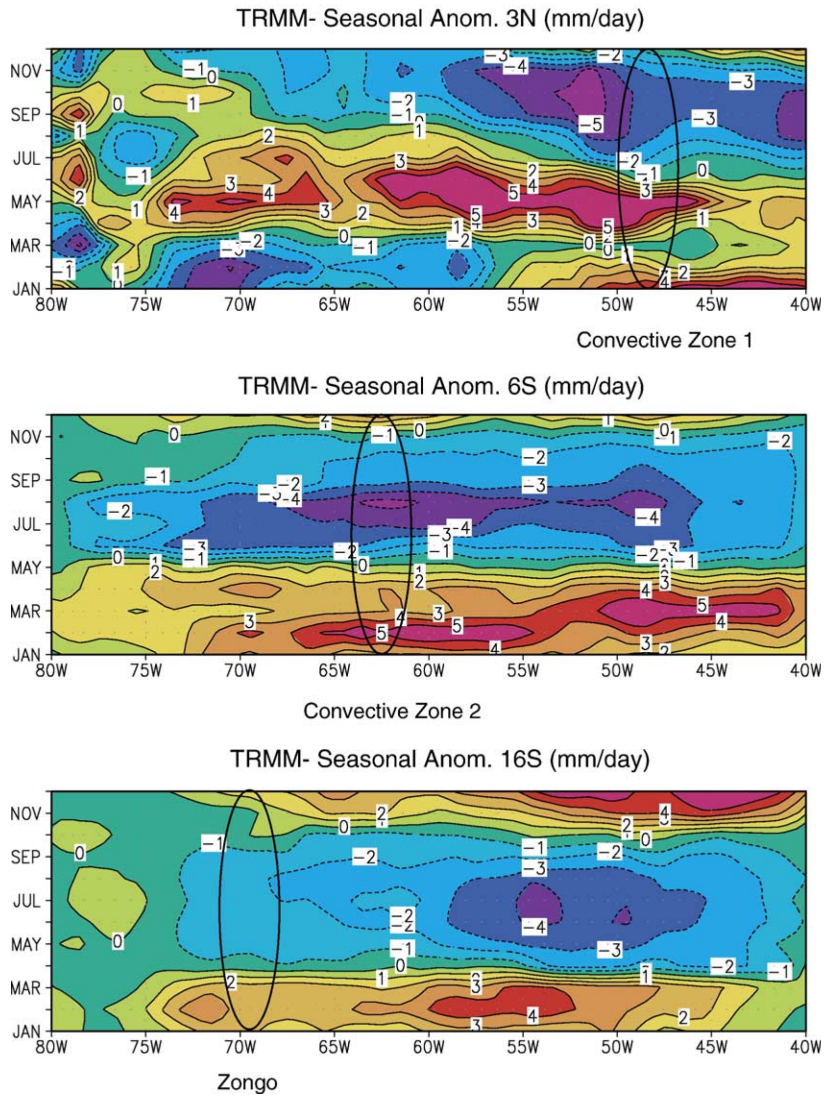

Fig. 7. Latitude–time diagram with TRMM precipitation seasonal cycle (deviations between the mean seasonal cycle and the annual mean of the mean seasonal cycle) averaged between September 1999 and March 2004 (mm/day), eastwards of the cordillera Real (40–80°W) at 16°S, 6°S and 3°N (latitudes intercepting both backtrajectories and convective zones). The convective zones 1 and 2 and the Zongo Valley locations are indicated.

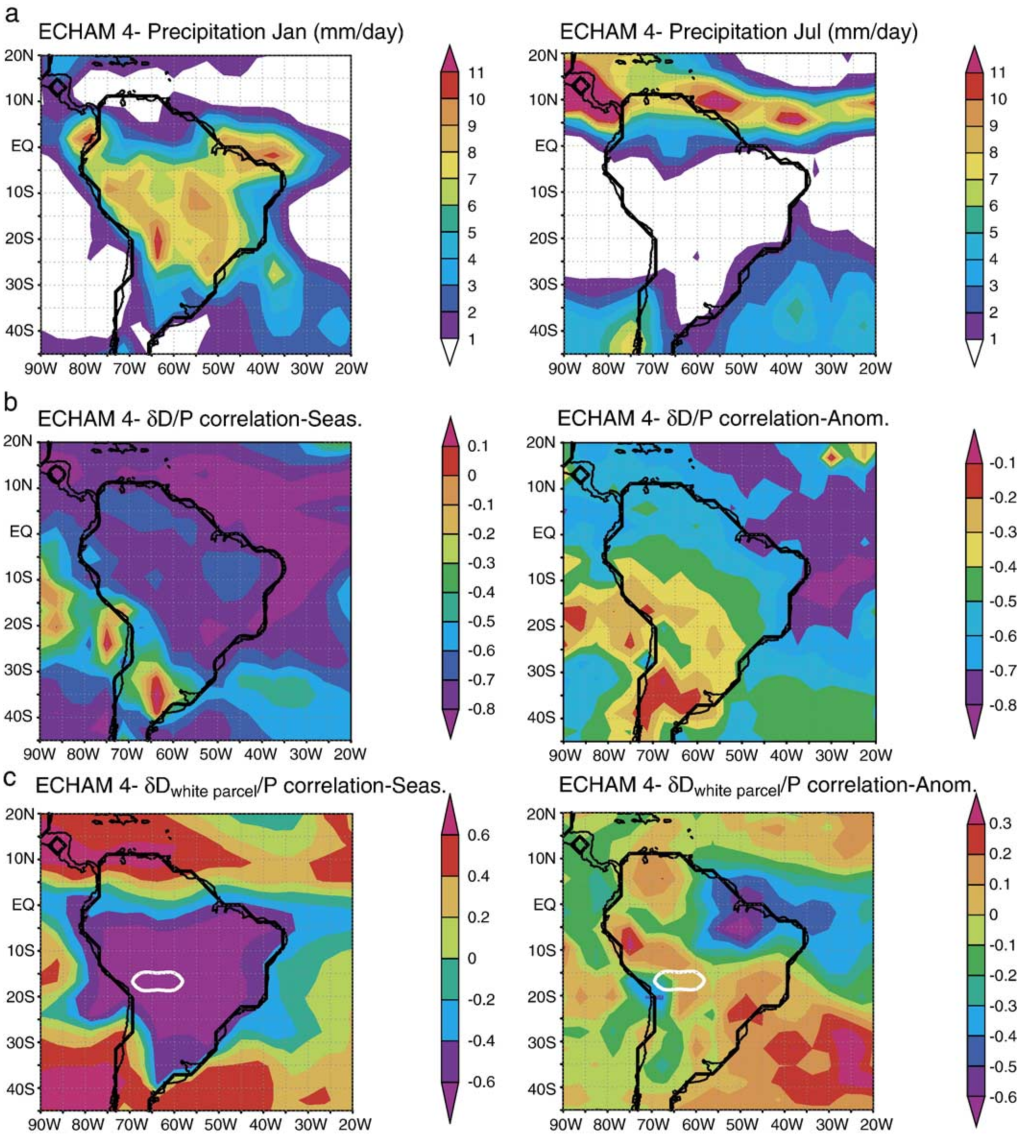

Fig. 8. Maps (20°N–45°S/20–90°W) derived from the 92-yr simulation from ECHAM-4 T30 showing (a) precipitation (mm/day) for January and July; (b) temporal correlation (r) between monthly isotopic composition (δD) of precipitation and precipitation amount at each grid point at seasonal (Seas.) and interannual (Anom.) time scale; (c) temporal correlation (r) between isotopic composition (δD) of precipitation averaged over a small region at the base of the Andes (14°S–18°S; 58–68°W) (white parcel) and precipitation amount at each grid point at seasonal (Seas.) and interannual (Anom.) time scale.

precipitation seasonal cycle is shown for different latitudes intercepting the major convective zones overflown by air masses. Moreover, Fig. 7 shows that the maximum of precipitation in the Zongo Valley occurs between January and March whereas in the convective zones 1 and 2, we observe a double peak in δ for precipitation in January and between March and April. This might be the explanation for the W-shape isotopic minimum we observe within the wet season in the valley.

Finally, we directly compare temporal δD_{Zongo} variations with TRMM precipitation although the later is only available until March 2004. We average TRMM precipitation over the 15–20°S/61–66°W region for the Zongo Valley and over the 5°N–18°S/35–70°W region for Amazonia (Table 2). Again, the correlation is better with Amazon precipitation (0.64 versus 0.55). We obtain similar covariances by slightly modifying the size of the Amazon region (±5° of latitude or longitude).

To offer support to our observations, we also compare δD_{Zongo} with another proxy of deep convection: Outgoing Longwave Radiation (OLR). OLR is regularly used to locate areas of deep tropical convection and as a proxy for precipitation by identifying the presence of cold cloud tops [29]: low OLR values correspond to cold and high clouds which denotes enhanced convection and an inverse relationship generally holds between OLR and convection.

The data used in this study are from the National Oceanic and Atmospheric Administration (NOAA) polar-orbiting satellites [30]. They are available at 2.5° latitude/longitude resolution and, in contrast to IAEA/GNIP precipitation, OLR data have the advantage of being spatially homogeneous and of common length of observations (September 1999–August 2004).

To easily compare with previous correlations based on mean seasonal cycle calculations, we first calculate a mean OLR seasonal cycle in both the Zongo (15–20°S/61–66°W) and the Amazon (5°N–18°S/35–70°W) regions as defined previously. Similarly to previous results, the δD_{Zongo}/Amazon OLR correlation (0.70, $p<0.001$) is fairly better than the δD_{Zongo}/Zongo OLR (0.47, $p>0.1$) (Table 2). If we focus only on OLR averaged over the CZ1 (5°N–5°S/45–53°W), the correlation is found to increase to 0.90. Again, the CZ1 seems to be a key zone in controlling δD_{Zongo} although air masses are southern during wintertime.

At last, we examine the temporal correlations of δD_{Zongo} with Amazon OLR and Zongo OLR from September 1999 to August 2004. They are of 0.52 and 0.32 respectively, supporting again the importance of remote rainout (Table 2).

The main point arising from this section is that seasonal variations of δD_{Zongo} can be reasonably understood not simply as a record of local rainout but as a record of the degree of rainout upstream the valley with an emphasized role of the regions of large scale convective activity over the Amazon basin.

2.1.3. Interannual variability—Atmospheric General Circulation Model (AGCM) simulation

In this section, we examine the climate controls on δD_{Zongo} at the interannual time scale. It is important, however, to keep in mind that our record covers only 5 yr and does not include any strong ENSO events that dominate the interannual variability of climate over tropical South America.

Our analyses are based on anomalies with the seasonal cycle removed by subtracting the long-term monthly mean from individual monthly values. The correlations between $\delta D_{Zongo\text{-}anom}$ and local precipitation and Amazon OLR and TRMM precipitation anomalies are found to be insignificant ($r^2<0.1$) offering no support for a control of $\delta D_{Zongo\text{-}anom}$ by the amount effect and the degree of air masses distillation. However, it may not be useful to examine interannual variations over a time period where the ENSO-related precipitation variability is absent. Actually, interannual variability of Amazon precipitation is mainly paced by ENSO [31,32] so that $\delta D_{Zongo\text{-}anom}$ could be mainly driven by precipitation variability upstream nonetheless. Indeed, some recent studies show a strong impact of important ENSO events in this valley. Ronchail and Gallaire [22] clearly show that the interannual variability of precipitation in the valley is paced by ENSO. A recent study dealing with heat and mass budget of the Glacier Zongo, up the Valley, shows a significant impact of the 1997–1998 El Niño [33].

To further investigate potential controls on $\delta D_{Zongo\text{-}anom}$ and also to test the robustness of our interpretation at seasonal time scale, we examine an AGCM simulation with water stable isotopes.

We use a 92-yr integration of the ECHAM-4 general circulation model [12,34] forced by observed SSTs and sea ice distributions in the T30 spectral resolution (corresponding to an approximate resolution of 3.75° lat. 3.75° long., ~420 km). The model quite accurately simulates both timing and spatial extent of precipitation over South America although it underestimates precipitation amount during the wet season (Fig. 8a). We first examine the correlation between the isotopic composition of precipitation (δD) and the precipitation amount in each grid point for both seasonal and interannual time scale (Fig. 8b). At the seasonal time scale, a significant anticorrelation is shown over the Amazon basin ($r<-0.7$) with lower r values at the base of the Andes (approximately −0.5/0.4). At the interannual time scale, the correlation between δD and precipitation is lower all over tropical South America. It strongly decreases southwesterly, indicating a decreasing control of local rainout on δD, and finally reaches an insignificant value at the base of the Andes ($r<-0.3$). The highest correlation is found over the CZ3 region where deep convection occurs. This basically reflects the strong local "amount effect" over the tropical Atlantic Ocean. Both maps support what we observe in our δ records that is a low and insignificant control of local rainout on δD_{Zongo} at the seasonal and interannual time scale respectively.

We now want to test the influence of the Amazon rainout on isotopic composition of precipitation falling at the base of the Andes. Thus, we examine the temporal correlation between the isotopic composition of precipitation (δD) regionally averaged between 14–18°S and 58–68°W (white parcel in Fig. 8c), excluding high elevations in the model grid and corresponding to the Northeast side of the Andes, and precipitation at each grid point for both seasonal and interannual time scale (Fig. 8c). As the T30 resolution does not offer an accurate representation of the elevation in the Andes (highest grid point reaches ~2000 m), our interpretations of the correlation maps account for the moisture transport pathways: we do not discuss significant correlations outside the domain where backtrajectories have been located. Moreover, we test the robustness of correlation patterns by slightly modifying the size of the white parcel (±1° in latitude, −5° westwards). At seasonal time scale, δD is similarly correlated with local and remote Amazon precipitation. Especially, a correlation tongue is found over the Northeast, at the edge of the continent towards the tropical Atlantic Ocean where CZ1 and CZ3 are located over the wet season. This clearly indicates that local rainout and degree of rainout upstream may be equally important to explain seasonal variations in δD. It is noteworthy that, as the white parcel width decreases westwards, the importance of the CZ1 increases compared to the rest of the Amazon basin ($\Delta r = -0.1$). At interannual time scale, δD is only significantly correlated with precipitation over the tropical Atlantic Ocean and the northern Amazon basin (conversely to our observations). Precipitation variations in those regions have been shown to be largely affected by ENSO, through its remote impact on tropical Atlantic climate variability via an “atmospheric bridge” [35] involving the Walker circulation changes [36]. This could explain the discrepancy with our observations not including ENSO variability. Thus, ECHAM-4 92-yr simulation suggests that interannual δD variability at the base of the Andes is significantly and indirectly paced by ENSO, as already suggested by Bradley et al. [10], Hoffmann [13] and Vuille et al. [16].

2.2. δD variations along the Zongo Valley

In this section, we are interested only in the isotopic depletion versus the elevation in the Zongo Valley.

From the lowest to the highest station, the mean isotopic depletion is of about 1.7‰/100 m ($r^2 = 0.96$). The absolute value of the δD versus altitude gradient never exceeds 2.5‰/100 m and is higher in the upper part of the valley (from 0.4 to 2.4 ‰/100 m in the valley). A pure Rayleigh model (open system) overestimates this gradient [37] whereas simulations using Rayleigh-based model accounting for convection or recycling (partly closed system, some condensate do not precipitate) reproduce quite well observations [38,39]. The mean δD-altitude gradient is within the range suggested by previous observation studies at those altitudes [37,38]. We note also that the seasonal cycle magnitude increases linearly with altitude from about 125‰ to 185‰ (Fig. 2).

The δD-precipitation slopes increase with altitude from −0.13 ‰/mm month^{-1} to −0.46‰/mm month^{-1} attaining a similar slope than other high elevation locations (the closest: La Paz, 4071 m: −0.45‰/mm month^{-1}). Assuming that the same water vapor parcel precipitates along this valley, a Rayleigh condensation predicts steeper slopes at high altitude where precipitation derives from vapor in more advanced stages of condensation. The low slope at the base of the valley (Harca, 1480 m) could reflect an important (non-fractionating) recycling of air masses over Amazonia. The later recharges air masses with more enriched vapor (same isotopic composition than precipitation) than the vapor left in the system and so counteracts the rainout effect and the δ/P slope is found to be lower than expected by air masses distillation alone.

Based on the calculated lapse rate and the mean isotopic depletion with altitude, the annual mean δD to temperature gradient along the Valley is of 3.5‰/°C. This value falls in the lower part of expected gradient for mid-latitude from a pure Rayleigh distillation, certainly because precipitation has experienced deeply convective activity leading to a system much more closed than a classical Rayleigh distillation [40].

A Rayleigh model predicts that water vapor becomes more and more depleted because of successive rainout. As the amount of vapor lost as precipitation is controlled by condensation temperature, the isotopic depletion depends eventually on the net cooling of the air mass. As already suggested by Gonfiantini et al. [38], using only 2-yr-long monthly data in Bolivia along a transect between the Bolivian Amazon basin and the Altiplano, we confirm here that the isotopic depletion during the air parcel uplift along the Zongo Valley might be described as a Rayleigh-based distillation providing that specific features of tropical water cycle being associated to a closed system are taken into account (convection for example).

3. Consequences for the Illimani ice core interpretation and conclusions

Our comparisons between δD_{Zongo} and local and regional climate illustrate the remote versus local influences of rainout and show that both factors impact δ at seasonal and interannual time scale. At seasonal time scale, local rainout is insufficient to explain δ variations and Amazon distillation of air masses can explain up to 90% of δ variance. The length of our δD records does not enable us to reliably discuss interannual variability. The use of a 92-yr simulation from ECHAM-4 model supports our observations at seasonal time scale and emphasizes the role of deep convective activity upstream the Andes on interannual δ variations. As already suggested by Hoffmann [13], Bolivian ice cores would record regional precipitation changes, highly connected to ENSO through Hadley-Walker atmospheric circulation. This suggests that Andean ice core information would contribute to the knowledge of the entire tropical bands highly teleconnected by the thermodynamic properties of the tropical troposphere [41].

The water vapor lifted up in the Andes can be described as a Rayleigh-based distillation provided that the system can be partially closed. The influence of this usually called "altitude effect", including important control by temperature, could be of primary importance when interpreting isotopic variations in ice core for past climate, as the glacial–interglacial δ^{18}O variation recorded in Illimani ice core (~7‰) [4]. Indeed, a change of temperature gradient between the Amazon basin and Andean summits in the past could have imprinted isotopic composition of past precipitation. It has been shown that the low to high altitude temperature differences was stronger during the LGM in the tropics. Recent estimates of tropical SSTs suggest that the mean zonal cooling in the tropics was somewhere between -2 and -3 °C [42–44]. Snow line depression studies on tropical mountains estimate a reduction between -5 and -6 °C at elevation of about 5 km in tropics [45]. Thus, a greater temperature gradient by 2 to 4 °C has been estimated at LGM between low and high elevations. Assuming that our calculated isotopic gradient versus temperature of 0.4‰/°C (deduced from δD/T gradient) holds true for the last glacial period and taking the weakest scenario for temperature gradient change ($\Delta T_{\text{base to top}}=+2$ °C), recently confirmed by Smith et al. [46] in Zongo Valley area, about 11% (2 * 0.4/7 ‰) of the LGM to present-day isotopic variation could arise from a stronger $\Delta T_{\text{base to top}}$ in the Andes at LGM. A recent study grouping 17 different AGCM simulations shows that mean global lapse rate (between 1000 and 6000 m) decrease at LGM is of order -0.02 to -0.03 °C/100 m because of the reduction of tropical SSTs resulting in a drier atmosphere and hence steeper lapse rates [47]. This study shows also that for the peculiar case of the Andes, it is quite difficult to conclude about lapse rate changes since the free atmospheric and along-slope lapse rate show opposite LGM to present-day variations (of about 0.02 to 0.03 °C/100 m for absolute value). Regardless, assuming the biggest simulated change in lapse rate, this only changes our previous estimate of 1%. Taking into account the $\delta D_{\text{Zongo}}/P_{\text{TRMM-Amazon}}$ slope, roughly translated into -0.06‰/mm for oxygen 18 (the δD_{Zongo}–Amazon precipitation slope (‰/mm) is higher than expected since we compare precipitation with isotopic composition of precipitation extracting at a higher degree of distillation), and based on an approximate modern average of about 1500 mm/yr of precipitation in Amazonia [48], the remaining 6.2‰ (7‰ -0.4‰/°C * 2 °C) for Illimani glacial–interglacial transition could be explained by wetter conditions over Amazonia of 7% during LGM. Thus, the major part of the glacial to Holocene isotopic transition at Illimani would reflect drier conditions (less distillation) along trajectories of the air masses over the Holocene, as concluded by Ramirez et al. [4].

Although we think that our study can be very useful for gaining insights into the interpretation of past δ variations, we also wish to emphasize that the previous discussion do not consider potential factors that might have a significant impact on δ change between LGM and the Holocene (hereafter, $\Delta\delta$). For example, we assume that our calibration holds true in the past when quantifying $\Delta\delta$ in terms of precipitation changes. We also assume that only precipitation affects $\Delta\delta$ whereas large scale reorganizations of the atmospheric circulations could have also impacted δ (southwards shift of ITCZ and induced changes in trajectories of the air masses and ocean moisture sources for example). Thus, past AGCM simulations and additional paleodata over the Andes are required to draw a robust conclusion about meteorological conditions in Amazonia during LGM and its changes during the glacial–interglacial transition.

We are also aware that our study deals with a very local network providing only 5-yr-long records and therefore we do not claim to propose here (1) a comprehensive calibration of the isotopic composition of modern Bolivian precipitation and (2) a comprehensive interpretation of isotopic variations in Andean ice cores. Our interpretation has to be confirmed with widespread and longer observations. Specifically, we need to record ENSO events to discuss the interannual variability. In this context, a large network over Bolivia (Peru) has been setting up for more than 4 yr (2 yr). We have also set up a network in Brasilia along the summertime air parcel pathways for 2 yr.

At last, to fully understand climate controls on Andean δ, we need to refer to high-resolution AGCM simulations with water stable isotopes. Actually, the resolution of ECHAM-4 T30 is really poor relative to the Andes elevation. In this context, water stable isotopes have been implemented in an atmospheric mesoscale model ($REMO_{iso}$) [49]. With such a model of a possible resolution of about 20 or 50 km, the various factors controlling for example the glacial to interglacial shift of the water isotopes could be estimated with much more confidence.

Acknowledgements

We deeply thank Rolando Fuertes and Tatiana Korobina for monitoring the precipitation network in the Zongo Valley and all the COBEE permanent observers for carefully collecting precipitation samples. We thank Sonia Falourd for her help in analyzing δD in precipitation. This paper has been improved by discussions with Bernard Pouyaud, Valérie Masson-Delmotte, Michel Stiévenard and two anonymous reviewers. This work was funded by IRD and Programme National d'Etude de la Dynamique du Climat (PNEDC-Amancay).

References

[1] L.G. Thompson, E. Mosley-Thompson, M.E. Davis, P.N. Lin, K.A. Henderson, J. Cole-Dai, J.F. Bolzan, K.B. Liu, Late glacial stage and Holocene tropical ice core records from Huascaran, Peru, Science 269 (1995) 46–50.

[2] L.G. Thompson, M.E. Davis, E. Mosley-Thompson, T.A. Sowers, K.A. Henderson, V.S. Zagorodnov, P.N. Lin, V.N. Mikhalenko, R.K. Campen, J.F. Bolzan, J. Cole-Dai, B. Francou, A 25,000-year tropical climate history from Bolivian ice cores, Science 282 (1998) 1858–1864.

[3] L.G. Thompson, E. Mosley-Thompson, K.A. Henderson, Ice-core palaeoclimate records in tropical South America since the Last Glacial Maximum, J. Quat. Sci. 15 (2000) 377–394.

[4] E. Ramirez, G. Hoffmann, J.D. Taupin, B. Francou, P. Ribstein, N. Caillon, F.A. Ferron, A. Landais, J.R. Petit, B. Pouyaud, U. Schotterer, J.C. Simoes, M. Stievenard, A new Andean deep ice core from Nevado Illimani (6350 m), Bolivia, Earth Planet. Sci. Lett. 212 (2003) 337–350.

[5] J. Jouzel, F. Vimeux, N. Caillon, G. Delaygue, G. Hoffmann, V. Masson-Delmotte, F. Parrenin, Magnitude of isotope/temperature scaling for interpretation of central Antarctic ice cores, J. Geophys. Res. 108 (2003), doi:10.1029/2002JD002677.

[6] EPICA Community Members, Eight glacial cycles from an Antarctic ice core, Nature 429 (2004) 623–628.

[7] W. Dansgaard, Stables isotopes in precipitation, Tellus XVI (1964) 436–447.

[8] K. Rosanski, L. Araguas-Araguas, R. Gonfiantini, Relation between long-term trends of oxygen-18 isotope composition of precipitation and climate, Science 258 (1992) 981–985.

[9] K. Rosanski, L. Araguas-Araguas, Spatial and temporal variability of stable isotope composition of precipitation over the South American continent, Bull. Inst. Fr. Etudes Andines 24 (1995) 379–390.

[10] R.S. Bradley, M. Vuille, D. Hardy, L.G. Thompson, Low latitude ice cores record Pacific sea surface temperatures, Geophys. Res. Lett. 30 (2003), doi:10.1029/2002GL016546.

[11] D.R. Hardy, M. Vuille, R.S. Bradley, Variability of snow accumulation and isotopic composition on Nevado Sajama, Bolivia, J. Geophys. Res. 108 (2003), doi:10.1029/2003JD003623.

[12] G. Hoffmann, E. Ramirez, J.D. Taupin, B. Francou, P. Ribstein, R. Delmas, H. Dürr, R. Gallaire, J. Simoes, U. Schotterer, M. Stievenard, M. Werner, Coherent isotope history of Andean ice cores over the last century, Geophys. Res. Lett. 30 (2003) 1179–1184.

[13] G. Hoffmann, Taking the pulse of the tropical water cycle, Science 301 (2003) 776–777.

[14] D. Noone, I. Simmonds, Associations between δ^{18}O of water and climate parameters in a simulation of atmospheric circulation for 1979–95, J. Clim. 15 (2002) 3150–3169.

[15] M. Vuille, R.S. Bradley, M. Werner, R. Healy, F. Keimig, Modeling δ^{18}O in precipitation over the tropical Americas: 1. Interannual variability and climatic controls, J. Geophys. Res. 108 (2003), doi:10.1029/2001JD002038.

[16] M. Vuille, R.S. Bradley, R. Healy, M. Werner, D.R. Hardy, L.G. Thompson, F. Keimig, Modeling δ^{18}O in precipitation over the tropical Americas: 2. Simulation of the stable isotope signal in Andean ice cores, J. Geophys. Res. 108 (2003), doi:10.1029/2001JD002039.

[17] J.R. Lawrence, S.D. Gedzelman, Tropical ice core isotopes: do they reflect changes in storm activity? Geophys. Res. Lett. 30 (2003) 1072–1076.

[18] J.R. Lawrence, S.D. Gedzelman, D. Dexheimer, H.-K. Cho, G.D. Carie, R. Gasparini, C.R. Anderson, K.P. Bowman, M.I. Biggerstaff, The stable isotopic composition of water vapor in the tropics, J. Geophys. Res. 109 (2004), doi:10.1029/2003JD004046.

[19] E. Salati, A.D. Olio, E. Matsui, J.R. Gat, Recycling of water in the Amazon Basin: an isotopic study, Water Resour. Res. 15 (1979) 1250–1258.

[20] J.R. Gat, E. Matsui, Atmospheric water balance in the Amazon Basin: an isotopic evapotranspiration model, J. Geophys. Res. 96 (1991) 13179–13188.

[21] B. Pouyaud, P. Ribstein, R. Gallaire, P. chevallier, Y. Caballero, E. Berthier, Régimes hydrologiques des hauts bassins nivo-glaciaires boliviens et variabilite pluviométriques des vallées andines en conditions El Nino et La nina, in: Manaus 99-Hydrological and Geochemical Processes in Large Scale River Basins, IRD-ANEEL Symp. Proc., 1999, CD-Rom 1–8.

[22] J. Ronchail, R. Gallaire, Enso and rainfall along the Zongo valley (Bolivia), from the Altiplano to the Amazon basin, Int. J. Climatology (submitted for publication).

[23] IAEA/WMO (2004). Isotope Hydrology Information System. The ISOHIS Database. Available online at: http://isohis.iaea.org.

[24] E. Kalnay, M. Kanamitsu, R. Kistler, W. Collins, D. Deaven, L. Gandin, M. Iredell, S. Saha, G. White, J. Woollen, Y. Zhu, M. Chelliah, W. Ebisuzaki, W. Higgins, J. Janowiak, K.C. Mo, C. Ropelewski, J. Wang, A. Leetmaa, R. Reynolds, R. Jenne, D. Joseph, The NCEP/NCAR 40-Year reanalysis project, Bull. Am. Meteor. Soc. 77 (1996) 437–471.

[25] R. Garreaud, Cold air incursions over Subtropical South America: mean structure and dynamics, Mon. Weather Rev. 128 (2000) 2544–2559.

[26] C. Kummerow, J. Simpson, O. Thiele, W. Barnes, A.T.C. Chang, E. Stocker, R.F. Adler, A. Hou, R. Kakar, F. Wentz, P. Ashcroft, T. Kozu, Y. Hong, K. Okamoto, T. Iguchi, H. Kuroiwa, E. Im, Z. Haddad, G. Huffman, B. Ferrier, W.S. Olson, E. Zipser, E.A. Smith, T.T. Wilheit, G. North, T. Krishnamurti, K. Nakamura, The status of the Tropical Rainfall Measuring Mission (TRMM) after two years in orbit, J. Appl. Meteorol. 39 (2000) 1965–1982.

[27] G.J. Huffman, R.F. Adler, P.A. Arkin, A. Chang, R. Ferraro, A. Gruber, J. Janowiak, R.J. Joyce, A. McNab, B. Rudolf, U. Schneider, P. Xie, The Global Precipitation Climatology Project (GPCP) combined precipitation dataset, Bull. Am. Meteorol. Soc. 78 (1997) 5–20.

[28] P. Xie, P.A. Arkin, Global precipitation: a 17-year monthly analysis based on gauge observations, satellite estimates, and numerical model outputs, Bull. Am. Meteorol. Soc. 78 (1997) 2539–2558.

[29] P.A. Arkin, P.E. Ardanuy, Estimating climatic-scale precipitation from space: a review, J. Clim. 2 (1989) 1229–1238.

[30] A. Gruber, F. Krueger, The status of NOAA outgoing longwave radiation dataset, Bull. Am. Meteorol. Soc. 65 (1984) 958–962.

[31] R. Garreaud, P. Aceituno, Interannual rainfall variability over the South American Altiplano, J. Clim. 14 (2002) 2779–2789.

[32] J. Ronchail, G. Cochonneau, M. Molinier, J.L. Guyot, A. Goretti De Miranda Chaves, V. Guimaraes, E. de Oliveira, Interannual rainfall variability in the Amazon basin and seas surface temperatures in the equatorial Pacific and the tropical Atlantic Oceans, Int. J. Climatol. 22 (2002) 1663–1686.

[33] P. Wagnon, P. Ribstein, B. Francou, J.E. Sicart, Anomalous heat and mass budget of Glaciar Zongo, Bolivia, during the 1997/98 El Niño year, J. Glaciol. 47 (2001) 21–28.

[34] M. Werner, M. Heimann, Modeling interannual variability of water isotopes in Greenland and Antarctica, J. Geophys. Res. 107 (2002) 4001–4014.

[35] N.C. Lau, M.J. Nath, The role of the atmospheric bridge in linking tropical Pacific ENSO events to extratropical SST anomalies, J. Clim. 9 (1996) 2036–2057.

[36] J.C.H. Chiang, Y. Kushnir, S.E. Zebiak, Interdecadal changes in eastern Pacific ITCZ variability and its influence on the Atlantic ITCZ, Geophys. Res. Lett. 27 (2000) 3687–3690.

[37] H. Shugui, V. Masson-Delmotte, Q. Dahe, J. Jouzel, Modern precipitation stable isotope vs. Elevation gradients in the High Himalaya. Comment on "A new approach to stable isotope-based paleoaltimetry: implications for paleoaltimetry and paleohypsometry of the High Himalaya since the Late Miocene" by David B. Rowley et al., Earth Planet. Sci. Lett. 209 (2003) 395–399.

[38] R. Gonfiantini, M.A. Roche, J.C. Olivry, J.C. Fontes, G.M. Zuppi, The altitude effect on the isotopic composition of tropical rains, Chem. Geol. 181 (2001) 147–167.

[39] L. Tian, V. Masson-Delmotte, M. Stievenard, T. Yao, J. Jouzel, Tibetan plateau summer monsoon northward extent revealed by measurements of water stable isotopes, J. Geophys. Res. 106 (2001) 28081–28088.

[40] P. Ciais, J. Jouzel, Deuterium and oxygen 18 in precipitation: isotopic model, including mixed cloud processes, J. Geophys. Res. 99 (1994) 16793–16803.

[41] J.C.H. Chiang, A.H. Sobel, Tropical tropospheric temperature variations caused by ENSO and their influence on the remote tropical climate, J. Clim. 15 (2002) 2616–2631.

[42] A. Rosell-Melé, E. Bard, K.C. Emeis, P. Farrimond, J. Grimalt, P.J. Müler, R. Schneider, Project takes a new look at past sea surface temperatures, Eos Transactions, Am. Geophys. Union 79 (1998) 393–394.

[43] C. Songozini, E. Bard, F. Rostek, Tropical sea surface temperature during the last glacial period: a view based on alkenones in Indian Ocean sediments, Quat. Sci. Rev. 17 (1998) 1185–1201.

[44] A.C. Mix, A.E. Morey, N.G. Pisias, S.W. Hostetler, Foraminiferal faunal estimates of paleotemperature: circumventing the no-analog problem yields cool ice age tropics, Paleoceanography 14 (1999) 350–359.

[45] D. Rind, D. Peteet, Terrestrial conditions at the Last Glacial Maximum and CLIMAP sea surface temperature estimates: are they consistent? Quat. Res. 24 (1985) 1–22.

[46] J.A. Smith, G.O. Seltzer, D.L. Farber, D.T. Rodbell, R.C. Finkel, Early local last glacial maximum in the Tropical Andes, Science 308 (2005) 678–681.

[47] M. Kageyama, S.P Harrison, A. Abe-Ouchi, The depression of tropical snowlines at the Last Glacial Maximum: what can we learn from climate model experiments? Quat. Int. 138–139 (2005) 202–219.

[48] W.P. Cramer, P. Leemans, The IIASA Database for Mean Monthly Values of Temperature, Precipitation, And Cloudiness on a Global Terrestrial Grid, IIASA, 1991.

[49] K. Sturm, B. Langmann, G. Hoffmann, W. Stichler, Stable isotopes in precipitation: a regional circulation modelling approach, Hydrol. Process. (in press).